Mathematical Biosciences and Engineering

https://www.aimspress.com/journal/mbe

MBE, 23(4): 884–912.
DOI: 10.3934/mbe.2026035
Received: 16 December 2025
Revised: 20 January 2026
Accepted: 26 January 2026
Published: 02 March 2026

Research article

Impact of insecticides on bee ecosystems: A mathematical approach using piecewise smooth dynamical systems

Carlos Andrés Trujillo-Salazar* **and Oscar Emilio Molina-Díaz**

Facultad de Ingenierías y Ciencias Básicas, Corporación Universitaria Empresarial Alexander von Humboldt, Armenia 630004, Colombia

* **Correspondence:** Email: ctrujillo@cue.edu.co; Tel: +573194728873.

Abstract: Honey bees (*Apis mellifera*) are key pollinators in agroecological systems and are crucial to ensuring global food security. However, apiculture is currently facing a crisis due to the proliferation of pests and diseases, with the ectoparasitic mite *Varroa destructor* posing the most significant threat. By feeding on the hemolymph of honey bees, this mite reduces their lifespan and acts as a vector for lethal viruses, potentially leading to the collapse of the entire beekeeping ecosystem. In this context, we propose a novel mathematical model based on a nonlinear system of ordinary differential equations to describe the interaction between the honey bee population and the *Varroa destructor* mite population, along with the temporal evolution of honey production. The model identifies the equilibrium states and examines their biological feasibility and stability in relation to key ecological thresholds. Numerical simulations are then conducted to illustrate the system's dynamics and to interpret, from an agroecological perspective, the impact of chemical control applied to crops situated in close proximity to the beekeeping environment. Subsequently, a switching mechanism is incorporated into the mite population equation, transforming the system in a piecewise smooth model. This mechanism activates or deactivates chemical control, depending on whether the ratio of mites to bees exceeds a predefined critical threshold. This approach captures the abrupt transitions induced by technical monitoring in apicultural practice, providing a more realistic framework for representing discontinuous control strategies. This work thus enables the evaluation of the differential impact of chemical pressure arising from neighboring crops and from targeted mite control, demonstrating, within the framework of ecological theory, how such interventions influence a population's viability and the long-term sustainability of the apicultural ecosystem.

Keywords: Honey bees; *Varroa destructor* mite; honey production; piecewise smooth dynamical systems; integrated pest control

1. Introduction

It is vital to acknowledge the fundamental importance of honey bees (*Apis mellifera*) to contemporary agroecological systems, as they play an important role in pollinating both cultivated and wild plant species. It has been determined that their pollination activity is responsible for the reproduction of approximately 35% of global food production, including fruits, vegetables, nuts, and oilseeds that rely directly on entomophilous pollination [1]. From an economic perspective, the value of the ecosystem services provided by bees is estimated at hundreds of billions of dollars annually worldwide, representing an economic contribution that far exceeds the direct market value of beekeeping products such as honey, wax, propolis, and pollen [2]. From an ecological perspective, honey bees play a pivotal role in preserving the genetic diversity of plant species and maintaining the stability of natural ecosystems. Their function as ecological connectors facilitates the movement of genes among fragmented plant populations, thereby contributing to the preservation of biodiversity [3]. It is evident that the decline in question represents a threat of considerable breadth, with implications for food security, rural economic sustainability, and the integrity of natural ecosystems [4].

Global apiculture is currently facing an unprecedented crisis due to the increasing incidence of pests and diseases affecting honey bee colonies [5]. Among the many stressors jeopardizing the health of apicultural ecosystems are viral, bacterial, and fungal pathogens; the indiscriminate use of pesticides [6, 7]; seasonal changes [8]; and, particularly, the proliferation of ectoparasites that have reached pandemic dimensions [9]. This health crisis has resulted in the phenomenon known as colony collapse disorder (CCD), characterized by the sudden and massive disappearance of worker bees, leaving behind colonies with queens, brood, and food stores, but lacking the adult population necessary to maintain the apicultural ecosystem's functionality [10]. Annual colony losses have reached alarming levels in various regions of the world, with mortality rates in some cases exceeding 30% [11], producing devastating impacts on the beekeeping industry and on agricultural systems that depend on pollination.

Among the multiple threats faced by honey bee populations, varroosis, caused by the ectoparasitic mite *Varroa destructor*, has emerged as the most destructive and widespread disease in global beekeeping [9]. This arthropod, originally from Asia, where it naturally parasitizes the Asian honey bee *Apis cerana*, successfully adapted to *Apis mellifera* during the 20th century [12], spreading globally and establishing itself as a strictly dependent parasite that has drastically disrupted the population dynamics of Western honey bee colonies [13]. The reproductive cycle of *Varroa destructor* is highly synchronized with the development of bee brood: It invades brood cells shortly before capping and reproduces inside them, where the founding females feed on the hemolymph of developing pupae [14]. Furthermore, in its phoretic phase, the mites attach to adult bees to feed and disperse, weakening them by consuming hemolymph and fat body tissue, while also facilitating the transmission of viruses such as deformed wing virus (DWV) [9]. This parasitic relationship not only directly debilitates individual bees, reducing their body mass, longevity, and immune capacity, but also acts as a vector for lethal viral transmission, establishing a pathological complex that can lead to the total collapse of the colony within one to three years if effective control measures are not implemented [15].

It is important to emphasize that mathematical modeling has emerged as a fundamental tool for

understanding and predicting complex phenomena in agroecological systems [16], enabling the formal representation of key biological interactions, the identification of critical parameters, and the evaluation of intervention scenarios. In the context of population ecology and applied entomology, mathematical models facilitate the integration of multiple biological, environmental, and management variables [17], transforming dispersed empirical observations into coherent predictive systems that can guide decision-making in agricultural ecosystem management. Mathematical modeling has proven particularly useful in evaluating integrated pest management strategies [18], optimizing sustainable management practices, predicting the impacts of climate change on agricultural production [19], and assessing the economic implications of various intervention scenarios. These models allow for the exploration of complex temporal dynamics, analyzing the sensitivity to external perturbations, and the identification of critical thresholds that determine a system's stability or collapse [20].

Among the key biological interactions represented by mathematical models in population ecology are predator–prey and host–parasitoid relationships, which are widely used to describe trophic and parasitic dynamics in both natural and agroecological systems. In particular, several models have been developed to represent the host–parasite relationship between honey bees (*Apis mellifera*) and the mite *Varroa destructor*, providing a formal framework for analyzing the impact of parasitism on population dynamics and, consequently, on honey production [21–25].

Alternatively, piecewise smooth (PWS) dynamical systems represent a specialized class of mathematical models that are particularly well suited to describe biological phenomena characterized by abrupt changes in a system's behavior in response to variations in the environmental conditions or the intrinsic system parameters [26]. These models are defined by switching surfaces that partition the state space into disjoint regions, within which the system exhibits distinct dynamics. This structure makes it possible to capture sharp transitions between behavioral patterns that are common in real-world biological systems [27]. In the context of population ecology, piecewise smooth systems have proven especially useful in modeling threshold effects in population density [28], seasonal changes in vital rates [29], responses to environmental stressors [30], and transitions between alternative stable states in ecosystems [31].

The application of mathematical modeling through piecewise smooth dynamical systems to describe the interaction between *Varroa destructor* and honey bee populations, as well as honey production, constitutes an innovative approach that captures the threshold–dependent characteristics inherent in this host–parasite system. A mathematical model is then proposed in which the state variables are the bee population, the mite population, and the quantity of honey, incorporating distinct population dynamics for these components depending on critical infestation levels that trigger the implementation of control measures. The switching mechanism of the system is applied specifically to the equation describing the mite population, where a critical threshold is defined in terms of the ratio of mites to bees; once this threshold is exceeded, insecticide-based control is automatically activated, abruptly altering the parasite's population dynamics. This mathematical framework realistically captures the integrated management strategies commonly used in beekeeping, where miticide treatments are deployed in response to pre-established critical infestation levels. The structured model thus provides a means to assess the differential impact of external factors on honey bees, *Varroa destructor*, and honey production within apicultural ecosystems, accounting for both the natural dynamics of the host–parasite system and human intervention through chemical treatments. It

also enables the prediction of productive scenarios under varying intervention thresholds and the optimization of control strategies based on ecological criteria.

This paper is organized as follows. In Section 2, we propose a mathematical model consisting of a system of nonlinear first-order ordinary differential equations that describes the population dynamics of honey bees and *Varroa destructor*, along with the evolution of honey production as a productive (non–population) variable. A classical qualitative analysis is then conducted, including the identification of equilibrium points, their biological relevance, and the characterization of their local stability in terms of ecological thresholds, all formalized through propositions. Subsequently, numerical simulations in the form of three-dimensional phase portraits are presented to illustrate the analytical results and provide agroecological interpretations of the indirect effects on the apicultural system of exposure to insecticides applied in adjacent or neighboring crop fields, exposure that primarily affects bees but also alters mite dynamics and honey production. In Section 3, a switching function is introduced into the differential equation governing the mite population's dynamics. This function activates or deactivates chemical control depending on whether the mite-to-bee ratio exceeds a critical threshold, transforming the model into a piecewise smooth system. A Filippov analysis is then applied, identifying the switching surfaces, classifying crossing and sliding zones, determining the existence of a pseudo-equilibrium, and establishing its local stability. These results are complemented with numerical simulations illustrating scenarios that are consistent with monitoring-based beekeeping practices. Section 4 discusses the main findings, identifies the limitations of the study, and outlines potential directions for future research. Finally, the references used throughout the paper are provided.

2. Formulation, qualitative analysis, and simulations of the smooth model

2.1. Formulation of the smooth model

A host–parasitoid interaction is to be mathematically modeled using a system of nonlinear ordinary differential equations, where the roles of the host and parasitoid are played by the honey bee (*Apis mellifera*) and the mite *Varroa destructor*, respectively. Additionally, a third component is incorporated into the dynamics, which, although not a population in the strict sense, represents the quantity of honey.

The formulation of this model is based on the standard assumptions from population ecology, including the following. The dynamics take place over a finite time horizon without specifying the exact location, which could correspond to a single hive or an entire apiary; climatic conditions and region–specific environmental factors are assumed to not significantly alter the population dynamics; the populations exhibit overlapping generations, meaning that individuals of different ages coexist; the population is homogeneously distributed, rendering the spatial position irrelevant; and migration phenomena are not considered.

Let $A = A(t)$ denote the average number of honey bees at time t, $V = V(t)$ be the average number of *Varroa destructor* mites at time t, and $M = M(t)$ the average quantity of honey produced by the bees at time t. Accordingly, the derivatives $\frac{dA}{dt}$ and $\frac{dV}{dt}$ represent the temporal variation in the respective populations, while $\frac{dM}{dt}$ corresponds to the rate of change in the amount of honey at time t.

The construction of the model begins by assuming that the bee population follows a logistic pattern, with ε denoting the intrinsic growth rate and k the carrying capacity. Parasitism is described through a mass action term βAV, where β is the parasitism rate. It is further assumed that bees also

die due to stress-related factors at a rate μ, as well as from exposure to insecticides used in crops adjacent to the apicultural ecosystem, at a rate q_1. It is important to note that no explicit distinction is made between immature and adult bees, since *Varroa destructor* parasitizes both life stages, reproducing inside capped brood cells and feeding on adult bees during its phoretic phase. In accordance with these assumptions, the population dynamics of honey bees are modeled by the following differential equation:

$$\frac{dA}{dt} = \varepsilon A\left(1 - \frac{A}{k}\right) - \beta AV - \mu A - q_1 A.$$

The population of *Varroa destructor* mites does not exhibit independent intrinsic growth, as their survival depends entirely on their parasitic interaction with the host bees. Thus, the growth of the mite population is directly related to the success of parasitism, represented by the term βAV. However, not all parasitic events result in a direct increase in the mite population; for this reason, a biomass conversion factor σ is introduced. Mites die from two main causes: Natural death at a rate ω, and death caused by insecticides at a rate q_2, which differs from q_1. Therefore, the population dynamics of *Varroa destructor* mites are modeled by the following differential equation:

$$\frac{dV}{dt} = \sigma\beta AV - q_2 V - \omega V.$$

The amount of honey in the system is determined by three fundamental processes: Production, extraction, and consumption. It is assumed that honey production is proportional to the size of the bee population, with ρ representing the rate of honey production per bee per unit of time. Honey extraction by the beekeeper is modeled as a continuous process with a constant rate α. Additionally, bees themselves consume honey for their subsistence, particularly during periods of nectar scarcity or adverse environmental conditions. This consumption is modeled as being proportional to both the bee population and the available amount of honey, through the term δAM, where δ represents the rate of honey consumption per bee per unit of time. Consequently, the dynamics of quantity of honey are described by the following differential equation:

$$\frac{dM}{dt} = \rho A - \alpha M - \delta AM.$$

The system consisting of the differential equations above adopts the following form:

$$\begin{aligned}
\frac{dA}{dt} &= \varepsilon A\left(1 - \frac{A}{k}\right) - \beta AV - \mu A - q_1 A,\\
\frac{dV}{dt} &= \sigma\beta AV - q_2 V - \omega V,\\
\frac{dM}{dt} &= \rho A - \alpha M - \delta AM,
\end{aligned} \tag{2.1}$$

where all parameters are strictly positive. The system (2.1) describes, according to the assumptions above made, a host–parasitoid interaction between honey bees and *Varroa destructor* mite, while also incorporating the dynamics of honey production as a component associated with the bee population. This deterministic model aims to analyze the joint behavior of the interacting populations and honey production under varying environmental conditions, with particular emphasis on the indirect effects caused by the exposure of the apicultural system to insecticides applied for pest control in adjacent or neighboring agricultural fields. Such exposure primarily affects the bees but also has repercussions on the dynamics of the mite and the production of honey.

2.2. Qualitative analysis of the smooth model

To study the system (2.1), we analyze the conditions under which the populations of bees and mites may either coexist or go extinct, and how these conditions determine the evolution of honey production within the system. For this purpose, we apply the classical analysis of equilibrium points, which involves their identification and an evaluation of their stability. The equilibrium points of the system (2.1) are

$$\begin{aligned}
E_1 &= (0,0,0)\,,\\
E_2 &= \left(\frac{k\,(\varepsilon-\mu-q_1)}{\varepsilon},\,0,\,\frac{k\rho\,(\varepsilon-\mu-q_1)}{\alpha\varepsilon+k\delta\,(\varepsilon-\mu-q_1)}\right),\\
E_3 &= \left(\frac{q_2+\omega}{\sigma\beta},\,\frac{\varepsilon k\sigma\beta-\varepsilon q_2-\varepsilon\omega-\mu k\sigma\beta-q_1 k\sigma\beta}{k\beta^2\sigma},\,\frac{\rho\,(q_2+\omega)}{\alpha\beta\sigma+\delta\,(q_2+\omega)}\right).
\end{aligned}$$

The equilibria E_2 and E_3 can be expressed in terms of thresholds, as shown below:

$$E_2 = \left(\frac{k}{A_0}\,(A_0-1)\,,0,\frac{\rho}{\delta}\left(1-\frac{\alpha\varepsilon}{\alpha\varepsilon+k\delta\,(q_1+\mu)\,(A_0-1)}\right)\right),$$

where

$$A_0 = \frac{\varepsilon}{q_1+\mu}. \tag{2.2}$$

Therefore,

$$E_3 = \left(\frac{q_2+\omega}{\sigma\beta},\,\frac{\varepsilon}{\beta U}\,(U-1)\,,\,\frac{\rho\,(q_2+\omega)}{\alpha\beta\sigma+\delta\,(q_2+\omega)}\right),$$

with

$$U = \frac{k\beta\sigma\varepsilon}{k\beta\sigma\,(q_1+\mu)+\varepsilon\,(q_2+\omega)}. \tag{2.3}$$

The expressions (2.2) and (2.3) satisfy the inequality $A_0 > U$. Indeed,

$$A_0 = \frac{\varepsilon}{q_1+\mu} = \frac{k\beta\varepsilon\sigma}{k\beta\sigma(q_1+\mu)} > \frac{k\beta\varepsilon\sigma}{k\beta\sigma(q_1+\mu)+\varepsilon(q_2+\omega)} = U,$$

where these quantities represent the thresholds commonly used in population ecology studies, such as in [32], where a threshold of this nature is referred to as the *net reproduction rate*. In deterministic population growth models, the basic reproduction number A_0 is defined as the expected number of offspring produced by an individual over its lifetime [33]. In the context of honey bee colonies, the threshold in (2.2) should be interpreted as an effective population–level replacement measure rather than a literal individual offspring count. It summarizes the colony's reproductive capacity mediated by the queen and balanced by mortality processes, determining whether population losses can be compensated in the absence of the parasitoid. Proposition 1 establishes the necessary conditions, expressed in terms of the thresholds in (2.2) and (2.3), for the equilibria E_2 and E_3 to be biologically meaningful.

Proposition 1. *The biological feasibility of the equilibrium points E_2 and E_3 depends on the thresholds of* (2.2) *and* (2.3) *as follows:*

1. *If* $A_0 < 1$, *then* E_2 *is not biologically feasible.*
2. *If* $A_0 = 1$, *then* E_2 *collides with* E_1.
3. *If* $A_0 > 1$, *then* E_2 *is biologically feasible.*
4. *If* $U < 1$, *then* E_3 *is not biologically feasible.*
5. *If* $U = 1$, *then* E_2 *and* E_3 *collide.*
6. *If* $U > 1$, *then* E_3 *is biologically feasible.*

Proof. The validity of statements 1–3 follows directly from the coordinates of E_2. Similarly, 4 and 6 are verified by inspecting the second coordinate of E_3. To prove 5, it suffices to prove that if $U = 1$, then E_2 and E_3 coincide in each of their coordinates, which is immediate for the second coordinate. Moreover,

$$U = \frac{k\sigma\beta\varepsilon}{k\sigma\beta\left(q_1+\mu\right)+\varepsilon\left(q_2+\omega\right)} = 1 \Leftrightarrow \frac{k\left(\varepsilon-\mu-q_1\right)}{\varepsilon} = \frac{q_2+\omega}{\sigma\beta},$$

which guarantees the coincidence of the first coordinates. Finally, by substituting this equality into the third coordinate of E_2, we obtain

$$\frac{k\rho\left(\varepsilon-\mu-q_1\right)}{\alpha\varepsilon+k\delta\left(\varepsilon-\mu-q_1\right)} = \frac{\rho\left(\frac{\varepsilon(q_2+\omega)}{\beta\sigma}\right)}{\alpha\varepsilon+\delta\left(\frac{\varepsilon(q_2+\omega)}{\beta\sigma}\right)} = \frac{\rho(q_2+\omega)}{\alpha\beta\sigma+\delta(q_2+\omega)},$$

which coincides with the third coordinate of E_3.

Propositions 2–4 present a classical local stability analysis of the equilibrium points E_1–E_3, respectively, under the assumption that each of them is hyperbolic. The methodology used in each case consists of determining the sign of the eigenvalues of the Jacobian matrix J of the system (2.1), which is given by

$$J\left(A,V,M\right) = \begin{pmatrix} \varepsilon\left(1-\frac{A}{k}\right)-\frac{\varepsilon}{k}A-\beta V-\mu-q_1 & -\beta A & 0 \\ \sigma\beta V & \sigma\beta A-q_2-\omega & 0 \\ \rho-\delta M & 0 & -\alpha-\delta A \end{pmatrix}. \tag{2.4}$$

Proposition 2. *The stability of the trivial equilibrium point* $E_1 = (0,0,0)$ *depends on the threshold* A_0 *given in* (2.2) *as follows:*

1. *If* $A_0 < 1$, *then* E_1 *is locally and asymptotically stable.*
2. *If* $A_0 = 1$, *then* E_1 *is non-hyperbolic.*
3. *If* $A_0 > 1$, *then* E_1 *is unstable, of the saddle point type.*

Proof. The Jacobian matrix (2.4) evaluated at the equilibrium point E_1 is given by

$$J\left(0,0,0\right) = \begin{pmatrix} \varepsilon-\mu-q_1 & 0 & 0 \\ 0 & -q_2-\omega & 0 \\ \rho & 0 & -\alpha \end{pmatrix}.$$

Two of its eigenvalues are negative; in fact, $\lambda_1 = -\alpha < 0$ and $\lambda_2 = -q_2-\omega < 0$. The sign of the third eigenvalue depends on A_0, as shown below:

$$\lambda_3 = \varepsilon-\mu-q_1 = \left(\mu+q_1\right)\left(\frac{\varepsilon}{\mu+q_1}-1\right) = \left(\mu+q_1\right)\left(A_0-1\right).$$

Indeed, if $A_0 < 1$, then $\lambda_3 < 0$, so the equilibrium point E_1 is local and asymptotically stable. If $A_0 = 1$, then $\lambda_3 = 0$ and, consequently, the equilibrium point E_1 is non–hyperbolic. If $A_0 > 1$, then $\lambda_3 > 0$, so the equilibrium point E_1 is unstable of the saddle point type.

According to Proposition 1, the stability analysis of the equilibrium points E_2 and E_3 is only relevant when $A_0 > 1$ and $U > 1$, respectively, as these conditions ensure that the corresponding points are biologically feasible. Under these assumptions, the local stability of E_2 and E_3 is analyzed in Propositions 3 and 4, respectively, which are presented below.

Proposition 3. *If $A_0 > 1$ and*

1. *$U < 1$, the equilibrium point E_2 is local and asymptotically stable;*
2. *$U = 1$, then E_2 is non–hyperbolic;*
3. *$U > 1$, then the equilibrium point E_2 is unstable of the saddle point type.*

Proof. It is important to recall, according to Proposition 1, that the equilibrium point E_2 is biologically feasible if $A_0 > 1$. Under this condition, the Jacobian matrix (2.4) is evaluated at the equilibrium point E_2, yielding the following eigenvalues:

$$\begin{aligned}
\lambda_1 &= -(q_1 + \mu)(A_0 - 1), \\
\lambda_2 &= -\frac{1}{\varepsilon}(\alpha\varepsilon + k\delta(q_1 + \mu)(A_0 - 1)), \\
\lambda_3 &= \frac{k\beta\sigma}{U}(U - 1).
\end{aligned}$$

Given that $A_0 > 1$ and all model parameters are positive, it follows directly that $\lambda_1 < 0$ and $\lambda_2 < 0$. Therefore, the nature of the equilibrium point E_2 is completely determined by the sign of the third eigenvalue λ_3, which, in turn, depends on the threshold U as follows:

- If $U < 1$, then $\lambda_3 < 0$, and since all three eigenvalues are negative, the equilibrium point E_2 is locally asymptotically stable.
- If $U = 1$, then $\lambda_3 = 0$, so E_2 is non-hyperbolic.
- If $U > 1$, then $\lambda_3 > 0$, and since two eigenvalues are negative and one is positive, the equilibrium point E_2 is unstable of the saddle type.

Remark. *The threshold A_0 defined in* (2.2) *depends on three parameters, among which q_1, representing the mortality rate of honey bees due to exposure to insecticides used in crops adjacent to the beekeeping ecosystem, is the only one that can be directly regulated through management practices by the beekeeper. In fact, with appropriate agroecological strategies, this parameter can be significantly reduced or even eliminated. Beyond its practical relevance, q_1 is also a key parameter for the qualitative analysis of the system. Indeed, the equilibrium analysis reveals three critical values of q_1 that lead to changes in the stability of the equilibria of the system* (2.1)*. The first of these is associated with the loss of hyperbolicity of the trivial equilibrium E_1, which occurs under the following condition:*

$$A_0 = \frac{\varepsilon}{q_1 + \mu} = 1 \Leftrightarrow q_1 = \varepsilon - \mu = q_1^*. \tag{2.5}$$

Another critical value of q_1 is obtained by considering the loss of hyperbolicity of the equilibrium E_2, which occurs when

$$U = \frac{k\sigma\beta\varepsilon}{k\sigma\beta\left(q_1+\mu\right)+\varepsilon\left(q_2+\omega\right)} = 1 \Leftrightarrow q_1 = \varepsilon - \mu - \frac{\varepsilon(q_2+\omega)}{k\beta\sigma} = q_1^* - \frac{\varepsilon(q_2+\omega)}{k\beta\sigma} = q_1^{**}. \tag{2.6}$$

Finally, the stability of equilibrium E_3 depends on the critical value

$$q_1^{***} = \varepsilon - \mu - \frac{\varepsilon(q_2+\omega)}{k\beta\sigma} - \frac{\varepsilon^2(q_2+\omega)}{4k^2\beta^2\sigma^2} = q_1^{**} - \frac{\varepsilon^2(q_2+\omega)}{4k^2\beta^2\sigma^2}, \tag{2.7}$$

as established in Proposition 4. It is important to note, according to (2.5)–(2.7)*, the hierarchy among the critical values of q_1 is as follows: $q_1^{***} < q_1^{**} < q_1^*$.*

Proposition 4. *If $U > 1$ and*

1. *$q_1 \geq q_1^{***}$, then the equilibrium point E_3 is a local node and is asymptotically stable.*
2. *$q_1 < q_1^{***}$, then the equilibrium point E_3 is a local spiral point and is asymptotically stable.*

Proof. It is important to remember, according to Proposition 1, that the equilibrium point E_3 is biologically feasible if $U > 1$. Under this condition, the Jacobian matrix (2.4) is evaluated at the equilibrium point E_3 and the following eigenvalues are obtained:

$$\begin{aligned}
\lambda_1 &= -\frac{\alpha\beta\sigma + \delta\left(q_2+\omega\right)}{\beta\sigma},\\
\lambda_2 &= -\frac{1}{2k\beta\sigma}\left(\varepsilon\left(q_2+\omega\right) + \sqrt{\varepsilon^2\left(q_2+\omega\right)^2 - \Delta}\right),\\
\lambda_3 &= -\frac{1}{2k\beta\sigma}\left(\varepsilon\left(q_2+\omega\right) - \sqrt{\varepsilon^2\left(q_2+\omega\right)^2 - \Delta}\right),
\end{aligned}$$

where

$$\Delta = 4k\beta\sigma\left(q_2+\omega\right)\left(k\sigma\beta\left(q_1+\mu\right)+\varepsilon\left(q_2+\omega\right)\right)\left(U-1\right).$$

Given that all model parameters are positive, it follows that $\lambda_1 < 0$. However, the remaining two eigenvalues may be either real or complex, depending on the discriminant. First, under the assumption that $\varepsilon^2\left(q_2+\omega\right)^2 - \Delta \geq 0$, it is clear that $\lambda_2 < 0$ and since $U > 1$ implies that $\Delta > 0$, then

$$\varepsilon\left(q_2+\omega\right) - \sqrt{\varepsilon^2\left(q_2+\omega\right)^2 - \Delta} > 0,$$

and thus $\lambda_3 < 0$. Second, if $\varepsilon^2\left(q_2+\omega\right)^2 - \Delta < 0$, then $\lambda_2, \lambda_3 \in \mathbb{C}$, and it is evident that the real part of λ_2 equals the real part of λ_3, both of which are negative. These conditions rule out the possibility of purely imaginary eigenvalues and, consequently, the equilibrium point E_3 cannot be a center. In conclusion, when E_3 has biological meaning, it is a locally asymptotically stable equilibrium point. The only remaining task is to determine whether it is a node (when the discriminant is non-negative) or a spiral (when the discriminant is negative). For this purpose, the discriminant is rewritten as follows:

$$\varepsilon^2\left(q_2+\omega\right)^2 - \Delta = \left(q_2+\omega\right)\left(4k^2\beta^2\sigma^2(\mu+q_1-\varepsilon) + 4k\beta\varepsilon\sigma(q_2+\omega) + \varepsilon^2(q_2+\omega)\right).$$

The equilibrium point E_3 is a local node and asymptotically stable if

$$4k^2\beta^2\sigma^2(\mu + q_1 - \varepsilon) + 4k\beta\varepsilon\sigma(q_2 + \omega) + \varepsilon^2(q_2 + \omega) \geq 0,$$

or, equivalently, if

$$q_1 \geq \varepsilon - \mu - \frac{\varepsilon(q_2 + \omega)}{k\beta\sigma} - \frac{\varepsilon^2(q_2 + \omega)}{4k^2\beta^2\sigma^2},$$

which corresponds to the expression given in (2.7). In conclusion, the equilibrium point E_3 is a local node and is asymptotically stable if $q_1 \geq q_1^{***}$ and is a local spiral and asymptotically stable if $q_1 < q_1^{***}$.

2.3. Numerical simulations of the smooth model

To illustrate the stability results established in Propositions 2–4, numerical simulations of the system (2.1) are made using an integration algorithm in MATLAB and the parameter values listed in Table 1. These values were selected solely for illustrative purposes and do not necessarily reflect real-world conditions. It is noteworthy that the parameter q_1 is not assigned a fixed value in the table, as it will be systematically varied in the simulations. As previously established through expressions (2.5)–(2.7), this parameter plays a critical role in determining the nature and stability of the equilibrium points of the system.

Table 1. Description and numerical values of the parameters used in the simulations of system (2.1).

P[1]	Description	Value
ε	Bees' growth rate	0.6
k	Carrying capacity of the bee population	500
β	Parasitism rate	0.02
μ	Bee mortality rate due to stress factors	0.01
q_1	Bee mortality rate due to exposure to insecticides in adjacent crops	varies
σ	Biomass conversion rate	0.2
q_2	Death rate of mites due to insecticides	0.25
ω	Natural death rate of the mite	0.02
ρ	Honey production rate	0.7
α	Honey consumption rate by beekeepers	0.01
δ	Honey consumption rate by bees	0.02

[1] Parameter

Figure 1 displays the phase portrait of system (2.1) under the condition $q_1 > q_1^*$, which, according to expression (2.5), is equivalent to $A_0 < 1$. In this specific case, $q_1 = 0.65 > 0.59 = q_1^*$. In accordance with Proposition 1, under this condition, the only biologically meaningful equilibrium point is E_1, which is the only visible point in Figure 1 and is locally and asymptotically stable, as established in Proposition 2. The system dynamics are illustrated through three trajectories, each originating from distinct initial conditions and converging asymptotically toward the origin, thereby confirming the stability of the equilibrium point. Biologically, this behavior corresponds to the extinction of both the bee and mite populations ($A \to 0$ and $V \to 0$), along with the complete depletion of honey

production ($M \to 0$). In summary, Figure 1 represents an ecologically consistent scenario in which a high bee mortality rate, caused by exposure to insecticides applied to crops adjacent to the beekeeping ecosystem ($q_1 = 0.65$), inevitably leads to the collapse of the bee population and, consequently, to the disappearance of both the mites and honey production.

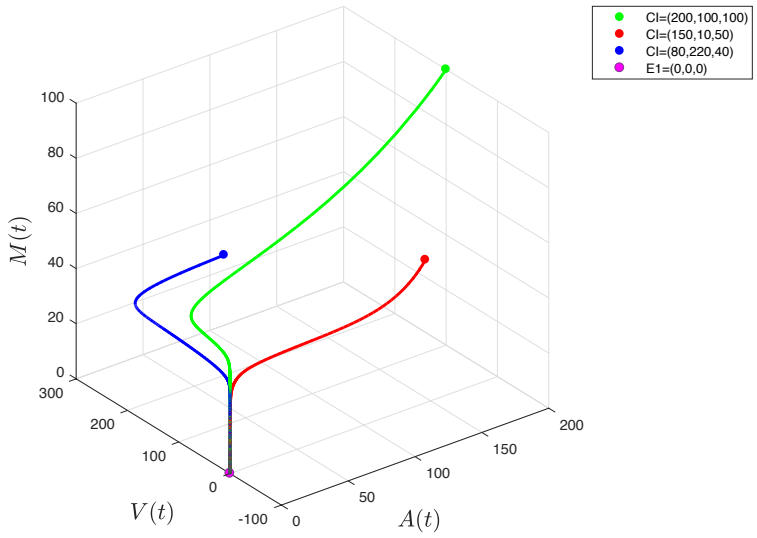

Figure 1. System phase portrait (2.1) with $q_1 = 0.65 > 0.59 = q_1^*$.

Figure 2 shows the phase portrait of system (2.1) under the condition $q_1^{**} < q_1 < q_1^*$, an inequality that, according to expressions (2.5) and (2.6), simultaneously guarantees that $A_0 > 1$ and $U < 1$. In particular, for $q_1 = 0.55$, these conditions imply, according to Proposition 1, that the equilibrium point E_2 is biologically feasible and is clearly identifiable in Figure 2, while the equilibrium point E_3 lacks biological meaning.

The system dynamics in this case exhibit greater complexity compared with the previously analyzed scenario, due to the presence of two biologically meaningful equilibrium points: E_1 and E_2. The stability analysis in Proposition 3 shows that E_2 is locally and asymptotically stable when $A_0 > 1$ and $U < 1$, as shown in Figure 2 by the convergence of the three trajectories toward this point, regardless of their initial conditions. Particularly notable is the red trajectory, which originates near the equilibrium point E_1 with the initial condition $(1, 1, 1)$ and diverges from it, corroborating its instability as established in Proposition 2 under the condition $A_0 > 1$. This divergence in asymptotic behavior confirms the existence of distinct attraction basins, separated by a separatrix that delineates the domains of influence of each equilibrium point.

From an agroecological perspective, the equilibrium point E_2 represents a state of population persistence in which both the bee population and honey production reach stable equilibrium values in the absence of mites. This behavior indicates that, under a scenario of moderate bee mortality due to exposure to insecticides applied to crops adjacent to the beekeeping ecosystem ($q_1 = 0.55$), the system can sustain a viable bee population and a steady level of honey production, provided that the initial conditions lie within the appropriate basin of attraction. The stability of E_2 suggests the long-term viability of the beekeeping ecosystem when the pressure from agrochemicals remains

within tolerable thresholds.

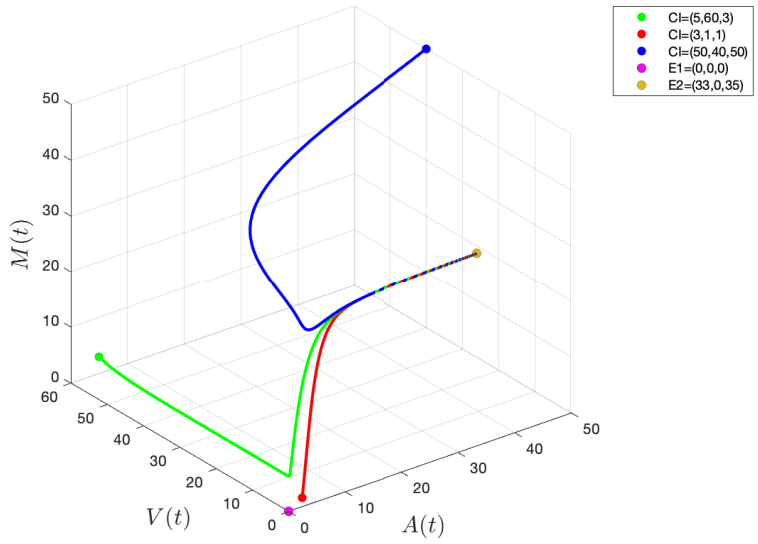

Figure 2. System phase portrait (2.1) with $q_1 = 0.55$, a value that satisfies the following relationship: $q_1^{**} = 0.509 < q_1 < 0.59 = q_1^*$.

Figure 3 shows the phase portrait of system (2.1) for the case $q_1 = 0.01 < q_1^{***} = 0.502925$. Since $q_1^{***} < q_1^{**} < q_1^*$, expressions (2.5) and (2.6) jointly ensure that $A_0 > 1$ and $U > 1$. Consequently, the equilibrium points E_2 and E_3 are biologically feasible, as stated in Proposition 1. In other words, under this scenario of low bee mortality due to insecticide exposure, the system exhibits dynamics with three biologically meaningful equilibrium points, all of which are clearly identifiable in Figure 3.

Under these conditions, the equilibrium points E_1 and E_2 are saddle–type unstable points, while the equilibrium point E_3 is a locally and asymptotically stable spiral, as established by Propositions 2–4, respectively. The nature of these equilibrium points is clearly illustrated in Figure 3, where it is observed that trajectories originating near E_1 and E_2 diverge from these points and approach E_3 asymptotically through spiral paths. These trajectories reflect the natural oscillations characteristic of certain host–parasitoid systems, indicating that the beekeeping ecosystem is capable of self-regulation and that the populations can coexist in a stable manner over the long term.

From an agroecological perspective, Figure 3 represents a dual-interpretation scenario. First, it is favorable for the beekeeper due to the minimal pressure exerted by insecticides applied to crops adjacent to the beekeeping ecosystem ($q_1 = 0.01$), which minimizes the impact of harmful anthropogenic factors. Furthermore, the stability of the equilibrium point E_3 represents a state of permanent coexistence for bees, mites, and a sustained level of honey production, which poses challenges from a beekeeping management standpoint. This scenario suggests that, under conditions of low anthropogenic interference, the beekeeping ecosystem can achieve an ecological balance in which the controlled presence of *Varroa destructor* mites does not compromise the viability of the bee population nor honey production, thereby representing a potentially desirable outcome from the perspective of sustainable apiculture. This situation raises important questions about the implications of implementing mite control strategies precisely when the ecosystem is in natural equilibrium,

considering that inappropriate interventions could disrupt the ecological balance achieved. In this context, the introduction of a chemical control mechanism applied directly to the pest is justified, where activation or deactivation depends on whether certain thresholds, defined in terms of the mite-to-bee ratio, are met. This leads to a more realistic mathematical model, in which the beekeeper's decisions are guided by ecological criteria derived from technical monitoring, and whose dynamics can be addressed using a piecewise smooth system.

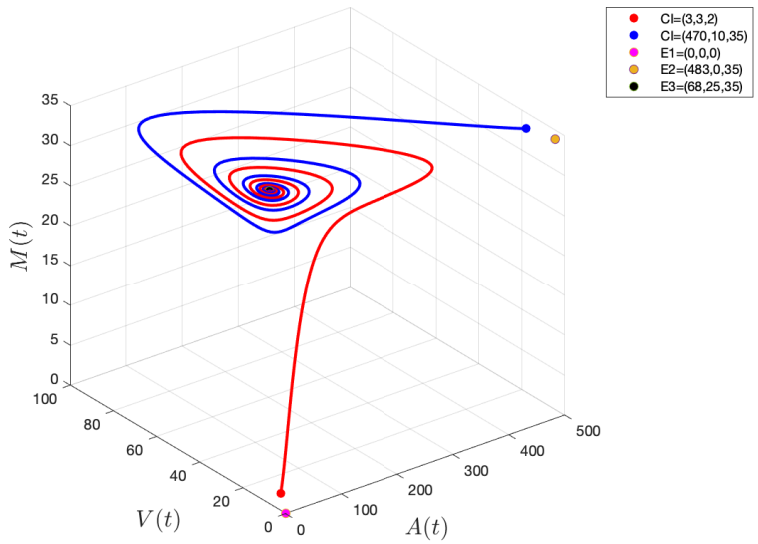

Figure 3. System phase portrait (2.1) with $q_1 = 0.01 < 0.502925 = q_1^{***}$.

3. Analysis of the piecewise smooth model

3.1. Piecewise smooth model

The mathematical model (2.1) provides a continuous and differentiable description of the population dynamics among honey bees, mites, and honey production under natural conditions. However, this classical approach presents certain limitations in accurately representing current beekeeping management practices, where chemical control interventions are implemented discontinuously in response to specific monitoring criteria. In practical apiculture, acaricide treatments are not applied continuously but are instead activated when infestation levels reach predetermined critical thresholds, generating abrupt changes in the system's population dynamics that cannot be adequately captured by classical models governed by differentiable differential equations.

The need to incorporate these punctual interventions, conditioned on the state of the system, arises from the recognition that the effective management of certain bee diseases, such as varroosis, is grounded in the concept of the economic injury threshold. According to this principle, chemical treatments are justified only when the cost of control is lower than the value of the avoided production losses. This principle, which has been firmly established in integrated pest management, implies the existence of a critical infestation level below which the colony can tolerate the presence of the mite without significantly compromising its productivity, and above which chemical intervention becomes

economically viable and biologically necessary [31]. The determination of this threshold is commonly based on the proportion of infested adult bees, an indicator that reflects both the intensity of the infestation and the imminent risk of colony collapse.

To incorporate such scenarios into the mathematical model, we propose the inclusion of a special function in the differential equation that describes the population dynamics of the mite *Varroa destructor*. This function is defined piecewise and governed by a switching term, which instantaneously modifies the population growth of the mite when a specific condition related to the infestation threshold is satisfied. Mathematically, this term is implemented by continuously evaluating the mite population and activating the effect of chemical control when it exceeds the pre-established threshold value [27].

The structure of the function governing the application of acaricides to the *Varroa destructor* population, which captures the switching mechanism in the system, is defined such that when the mite population exceeds a critical threshold, denoted by $\eta(V)$, the system evolves according to the natural dynamics of the original smooth model while incorporating an additional mortality term for the mite population, representing the lethal effect of the acaricide treatment. Conversely, if the infestation level remains below the threshold, no treatment is applied, and the mite population grows according to the intrinsic biological parameters of the host–parasite interaction. This modification transforms the system of ordinary differential equations into a piecewise smooth system, characterized by the presence of switching surfaces that divide the state space into regions with distinct dynamical behaviors [26, 34].

The mathematical implementation of the switching term requires the precise definition of the switching function, which must be capable of detecting the crossing of the infestation threshold and activating the control mechanism accordingly. This function is typically constructed using relational operators that compare the current proportion of infested bees to a predefined threshold value, generating a binary signal that determines the activation or deactivation of the chemical control term. This binary signal can be formally expressed using a characteristic function, also known as an indicator function. The inherent discontinuity of this function is the fundamental property that gives the model its piecewise smooth nature, enabling the coexistence of qualitatively different dynamic behaviors across regions of the state space [26].

The incorporation of the switching term into the model not only significantly enhances its biological realism and practical relevance but also introduces new mathematical complexities that enrich the dynamic analysis of the system. The presence of discontinuities in the vector field gives rise to the possibility of complex dynamic phenomena, including sliding motions along the switching surfaces [35]. These dynamic behaviors reflect biologically plausible situations, such as alternation between periods of natural infestation growth and episodes of intensive chemical control, or the stabilization of infestation levels near the intervention threshold through the intermittent application of treatments.

To begin with, we consider that $\mathbf{x} = (A, V, M)^T$ and the system of differential equations defined by

$$\dot{\mathbf{x}} = \begin{cases} \varepsilon A\left(1 - \dfrac{A}{k}\right) - \beta AV - \mu A - q_1 A \\ \sigma\beta AV - \eta q_2 V - \omega V \\ \rho A - \alpha M - \delta AM \end{cases}, \tag{3.1}$$

where

$$\eta = \begin{cases} 0 & \text{si} \quad V < \xi k \\ 1 & \text{si} \quad V > \xi k \end{cases}, \tag{3.2}$$

is the switching term, which can be interpreted using the characteristic function. It is activated when the number of mites exceeds the value ξk, where ξ represents an approved infestation threshold for the bee population and typically lies between 3% and 5%, according to the studies conducted in [9,36–39], and k denotes the carrying capacity of the apicultural ecosystem [36]. Therefore, the term ξk corresponds to a proportion of the total bee population.

At this point, it is pertinent to justify the switching concept. Recall that ξ denotes the allowable infestation threshold for the bee population and represents the critical tolerance level of the apicultural ecosystem to parasitism by the mite *Varroa destructor*. Values ranging between 3% and 5% reflect, respectively, the ecological limit preceding a population collapse, (namely, the point at which the colony's demographic compensation mechanisms reach saturation), and the threshold established in apicultural practice for integrated pest management interventions. Nevertheless, the parameter k represents the carrying capacity of the system, that is, the maximum sustainable population size given the constraints of the apicultural ecosystem. This capacity is determined by limiting factors such as the availability of trophic resources, the physical space available for brood development, and the colony's physiological capabilities in terms of thermoregulation and immunological defense.

Therefore, the term ξk represents the absolute critical population of mites that the apicultural ecosystem can withstand before qualitative changes in the system's dynamics are triggered. Mathematically, this is

$$\text{Critical threshold} = \xi k = (\text{critical proportion})(\text{total capacity}).$$

The ecological meaning of the switching term indicates that the system undergoes a change in its dynamic regime when the population of the mite *Varroa destructor* approaches or exceeds the quantity ξk, which entails the following biological implications.

- When $V < \xi k$ (that is, under low infestation levels), the apicultural ecosystem remains in a state of homeostasis, meaning that its ability to maintain a stable and continuous internal environment is preserved. In this regime, bees exhibit normal foraging, brood-rearing, and defensive behaviors; honey production is optimal; natural defense mechanisms are sufficient; and the impact of the mite on the bee population remains stable.
- If $V \approx \xi k$, the system enters a critical state in which the colony experiences physiological and behavioral stress, defensive responses are activated, honey production begins to decline, the colony's structure is altered, and vulnerability to secondary diseases increases.
- When $V > \xi k$ (that is, under a high-infestation scenario), the apicultural ecosystem enters a collapse dynamic characterized by accelerated bee mortality, reduced honey production, diminished reproductive capacity, and an increased risk of extinction.

It is precisely in this latter scenario that the inclusion of control mechanisms, either chemical or biological, becomes necessary to regulate the mite population. This intervention is incorporated into the model through the term $-\eta q_2 V$, where q_2 denotes the mite mortality rate induced by insecticides.

On this basis, we have the piecewise smooth system

$$\dot{\mathbf{x}} = \begin{cases} f_1(\mathbf{x}) & \text{si} \quad \mathbf{x} \in S_1 \\ f_2(\mathbf{x}) & \text{si} \quad \mathbf{x} \in S_2 \end{cases}, \tag{3.3}$$

where S_1, $S_2 \in \mathbb{R}^3$ are disjoint open sets defined as follows:

$$\begin{aligned} S_1 &= \left\{\mathbf{x} \in \mathbb{R}^3 : \ V < \xi k\right\}, \\ S_2 &= \left\{\mathbf{x} \in \mathbb{R}^3 : \ V > \xi k\right\}, \end{aligned}$$

which are separated by the switching plane

$$\Sigma = \left\{\mathbf{x} \in \mathbb{R}^3 : \ V = \xi k\right\} = \left\{\mathbf{x} \in \mathbb{R}^3 : \ V - \xi k = 0\right\}, \tag{3.4}$$

which can be expressed through the zero-level set of the smooth scalar field $H(\mathbf{x}) = V - \xi k$, which has a gradient $H_{\mathbf{x}}(\mathbf{x}) = (0, 1, 0)$, which clearly does not vanish in Σ.

Thus, we have the vector fields

$$f_1(\mathbf{x}) = \begin{cases} \varepsilon A\left(1 - \dfrac{A}{k}\right) - \beta AV - \mu A - q_1 A \\ \sigma\beta AV - \omega V \\ \rho A - \alpha M - \delta AM \end{cases} \tag{3.5}$$

and

$$f_2(\mathbf{x}) = \begin{cases} \varepsilon A\left(1 - \dfrac{A}{k}\right) - \beta AV - \mu A - q_1 A \\ \sigma\beta AV - q_2 V - \omega V \\ \rho A - \alpha M - \delta AM \end{cases} \tag{3.6}$$

which are defined in S_1 and S_2, respectively. Figure 4 shows the regions S_i and the vector fields f_i, $i = 1, 2$, which act in them, as well as the commutation plane Σ, which is colored blue.

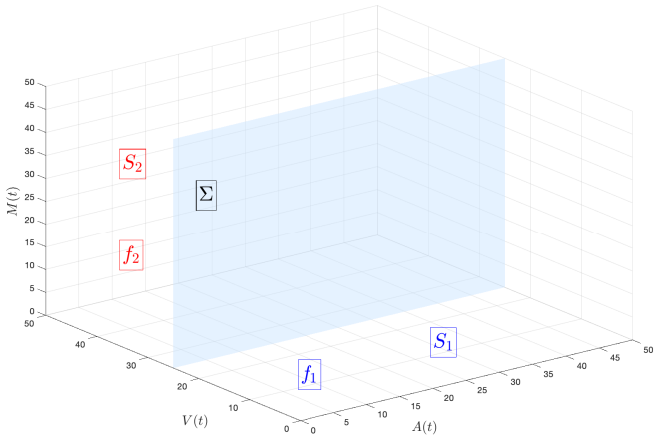

Figure 4. The switching plane Σ, defined in (3.4) and represented in blue, together with the vector fields f_i acting in each region S_i, for $i = 1, 2$. These regions and their respective fields correspond to the piecewise smooth system given in (3.3).

3.2. Analysis of the piecewise smooth model

The behavior of the trajectories of the nonsmooth system (3.3) is studied in a neighborhood of the switching surface Σ by applying the Filippov method [26]. To this end, the Lie directional derivative is required [40], which is defined by

$$\mathcal{L}_{f_i}H(\mathbf{x}) = \langle H_{\mathbf{x}}(\mathbf{x}), f_i(\mathbf{x})\rangle.$$

In general, the expressions $\mathcal{L}_{f_i}H(\mathbf{x})$, $i = 1, 2$, are referred to as normal components and indicate the direction in which the vector field f_i points at $\mathbf{x} \in \Sigma$. Thus, for those $\mathbf{x} \in \Sigma$ such that $\mathcal{L}_{f_i}H(\mathbf{x}) > 0$, the vector field f_i and the normal vector to the surface Σ point in the same direction. In contrast, if $\mathcal{L}_{f_i}H(\mathbf{x}) < 0$, then the vector field f_i and the normal vector to the surface Σ point in opposite directions [27, 41].

On this basis, the expression is defined as follows:

$$\sigma(\mathbf{x}) = \langle H_{\mathbf{x}}(\mathbf{x}), f_1(\mathbf{x})\rangle\langle H_{\mathbf{x}}(\mathbf{x}), f_2(\mathbf{x})\rangle = V^2(\sigma\beta A - \omega)(\sigma\beta A - q_2 - \omega),$$

which allows for the identification of crossing and sliding points on the switching surface. Initially, at the points $\mathbf{x}$ on Σ where $\boldsymbol{\sigma}(\mathbf{x}) > 0$, the vector fields exhibit a crossing behavior, since the normal components at those points share the same sign, causing both vector fields to point in the same direction. This set of points is called the crossing region and is denoted by Σ^c. Thus

$$\sigma(\mathbf{x}) = (\xi k)^2\,(\sigma\beta A - \omega)(\sigma\beta A - q_2 - \omega) > 0,$$

in the set

$$\Sigma^c = \left\{\mathbf{x} \in \Sigma :\ A < \frac{\omega}{\sigma\beta}\ \vee\ A > \frac{\omega + q_2}{\sigma\beta}\right\}.$$

Otherwise, at the points $\mathbf{x} \in \Sigma$ such that $\boldsymbol{\sigma}(\mathbf{x}) \leq 0$, one obtains the set of sliding points. At these points, the two normal components have opposite signs, causing the vector fields to point in opposite directions. This set is denoted by Σ^s and is defined as

$$\Sigma^s = \left\{\mathbf{x} \in \Sigma :\ \frac{\omega}{\sigma\beta} \leq A \leq \frac{\omega + q_2}{\sigma\beta}\right\}.$$

It should be noted that sliding occurs when there is disparity in the signs of the normal components. This occurs in the following configurations:

(a) $\langle H_{\mathbf{x}}(\mathbf{x}), f_1(\mathbf{x})\rangle < 0 < \langle H_{\mathbf{x}}(\mathbf{x}), f_2(\mathbf{x})\rangle$. This means that the vector fields f_1 and f_2 point outside the switching surface Σ. This set of sliding points forms the unstable sliding set and is denoted by Σ^{us}. It is also known as the scape set.

(b) $\langle H_x^{(1)}(\mathbf{x}), f_1(\mathbf{x})\rangle > 0 > \langle H_x^{(1)}(\mathbf{x}), f_2(\mathbf{x})\rangle$. In this case, the vector fields f_1 and f_2 point toward Σ. This set of sliding points forms the stable sliding set, which is also known as an attractor and is denoted by Σ^{ss}.

It is important to note that $\Sigma^s = \Sigma^{ss} \cup \Sigma^{us}$. In Figure 5, the set of crossing points Σ^c is shown in blue, while the sliding region Σ^s is depicted in yellow. Moreover, the system (3.3) exhibits only stable

sliding; therefore, in order for the first condition above, (namely, unstable sliding), to be satisfied, the following must occur:

$$\frac{\omega + q_2}{\sigma\beta} < A < \frac{\omega}{\sigma\beta},$$

which is not satisfied, since the parameters under consideration are positive.

It is worth mentioning that the set of points satisfying $\sigma(\mathbf{x}) = 0$ is known as the set of tangential points, which correspond to the points lying on the lines $A = \dfrac{\omega}{\sigma\beta}$ and $A = \dfrac{\omega + q_2}{\sigma\beta}$ on the plane $V = \xi k$. These lines define the boundary between the region of stable sliding and the crossing region, as illustrated in Figure 5.

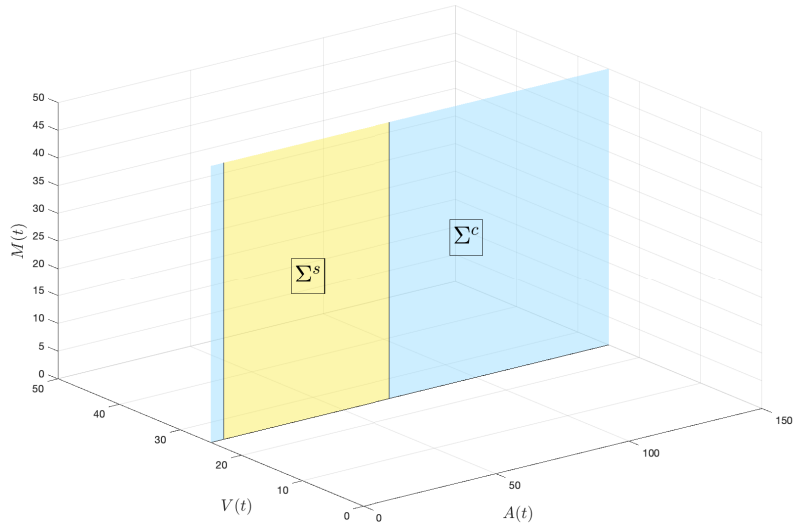

Figure 5. The switching surface Σ defined in (3.4) and the crossing zones Σ^c in blue, and the sliding zones Σ^s in yellow on this plane.

For $\mathbf{x} \in \Sigma$, it is possible to define a sliding vector field, also known as the Filippov system, as a convex combination of the vector fields adjacent to the switching surface Σ, a formulation commonly referred to as Filippov's convention [26, 27], given by

$$\dot{\mathbf{x}} = g(\mathbf{x}),$$

where

$$g(\mathbf{x}) = \lambda(\mathbf{x}) f_1(\mathbf{x}) + (1 - \lambda(\mathbf{x})) f_2(\mathbf{x}),$$

with

$$\lambda(\mathbf{x}) = \frac{\langle H_{\mathbf{x}}(\mathbf{x}),\ f_2(\mathbf{x})\rangle}{\langle H_{\mathbf{x}}(\mathbf{x}),\ f_2(\mathbf{x}) - f_1(\mathbf{x})\rangle}.$$

After some algebraic operations, we have

$$\lambda(\mathbf{x}) = 1 + \frac{\omega}{q_2} - \frac{\sigma\beta A}{q_2}.$$

Therefore,

$$\dot{\mathbf{x}} = g(\mathbf{x}) = \begin{cases} \varepsilon A\left(1 - \dfrac{A}{k}\right) - \beta A\xi k - \mu A - q_1 A \\ 0 \\ \rho A - \alpha M - \delta AM \end{cases}. \tag{3.7}$$

Since the sliding dynamics reduce to a two-dimensional system within the sliding region over the switching plane $V = \xi k$, which is parallel to the AM coordinate plane, the analysis is thus restricted to the following planar system:

$$\dot{\mathbf{x}} = g(\mathbf{x}) = \begin{cases} \varepsilon A\left(1 - \dfrac{A}{k}\right) - \beta A\xi k - \mu A - q_1 A \\ \\ \rho A - \alpha M - \delta AM \end{cases}. \tag{3.8}$$

In Filippov systems, it is possible to identify the existence of pseudo-equilibria, which are equilibria of the sliding vector field $g(\mathbf{x})$ lying on Σ^s, but are not equilibria of any of the original vector fields of the system [27]. In this case, two points are identified: $\mathbf{x_0} = (0, 0)$, which does not lie on the switching surface, and

$$\mathbf{x_1} = \left(k\left(1 - \frac{\beta\xi k + \mu + q_1}{\varepsilon}\right),\ \frac{\rho k\left(1 - \dfrac{\beta\xi k + \mu + q_1}{\varepsilon}\right)}{\alpha + \delta k\left(1 - \dfrac{\beta\xi k + \mu + q_1}{\varepsilon}\right)} \right). \tag{3.9}$$

Note that if $\xi = 0$ and the second component is taken as $V = \xi k$, the equilibrium point E_2 from the previous section is recovered. The system, however, has no singular sliding points, since these arise at $\mathbf{x} \in \Sigma$ when $\langle H_{\mathbf{x}}(\mathbf{x}),\ f_2(\mathbf{x}) - f_1(\mathbf{x})\rangle = 0$, which, in this case, reduces to

$$-q_2 V = 0,$$

an impossibility because, on Σ, we have $V = \xi k$.

Proposition 5. *The system* (3.3) *has a single pseudo–equilibrium given in* (3.9)*, which is local and asymptotically stable if* $\beta\xi k + \mu + q_1 < \varepsilon$.

Proof. To analyze the stability of the pseudo–equilibrium $\mathbf{x_1}$, the Jacobian matrix $Jg(\mathbf{x})$ is necessary, which is given as follows:

$$Jg(\mathbf{x}) = \begin{pmatrix} \varepsilon - \dfrac{2\varepsilon A}{k} - \beta\xi k - \mu - q_1 & 0 \\ \rho - \delta M & -\alpha - \delta A \end{pmatrix}.$$

Evaluating the pseudo-equilibrium $\mathbf{x_1}$ in $Jg(\mathbf{x})$, we obtain

$$Jg(\mathbf{x_1}) = \begin{pmatrix} \beta\xi k + \mu + q_1 - \varepsilon & 0 \\ \dfrac{\rho\alpha}{\alpha + \delta k\left(1 - \dfrac{\beta\xi k + \mu + q_1}{\varepsilon}\right)} & -\alpha - \delta k\left(1 - \dfrac{\beta\xi k + \mu + q_1}{\varepsilon}\right) \end{pmatrix}.$$

Since the matrix is lower triangular, its eigenvalues correspond to the entries on the main diagonal, i.e.,

$$\begin{aligned}\lambda_1 &= \beta\xi k + \mu + q_1 - \varepsilon,\\ \lambda_2 &= -\alpha - \delta k\left(1 - \frac{\beta\xi k + \mu + q_1}{\varepsilon}\right),\end{aligned}$$

from which it is clear that $\lambda_1 < 0$ and $\lambda_2 < 0$ if $\beta\xi k + \mu + q_1 < \varepsilon$. Therefore, under this condition, the pseudo–equilibrium $\mathbf{x_1}$ is local and asymptotically stable.

At this point, it is important to mention and synthesize, within this context, several key aspects that have been developed thus far. It is well known that the switching plane $V = \xi k$ divides the state space into two regions with distinct dynamics. In Region 1, defined by the set of points for which $V < \xi k$, the system operates without chemical control, and the apicultural ecosystem naturally manages the low presence of mites. In Region 2, where $V > \xi k$, the system operates under chemical control, and intervention through acaricides becomes necessary.

A trajectory crosses the switching plane when it intersects the plane $V = \xi k$ transversely, transitioning from one region to the other; that is, when the population of the mite exceeds the threshold ξk. When the crossing is upward (from Region 1 to Region 2), infestation surpasses the critical level and the chemical control protocol is activated. Ecologically, this indicates that the colony's natural defense mechanisms have been exceeded and human intervention is required to prevent collapse. Conversely, a downward crossing occurs when chemical control has successfully reduced the mite population below the threshold, leading to the deactivation of acaricide application. The colony then returns to a state in which its natural defenses are sufficient to keep the infestation under control.

It is well known that when a trajectory reaches the switching plane (more precisely, within the sliding region), it remains on it for a finite time interval rather than crossing it immediately; that is, the system is actively maintained at the exact threshold through intermittent control actions. Biologically, this has several implications. The mite population is maintained precisely at $V \approx \xi k$ through strategic and dosed applications of acaricides; the beekeeper implements adaptive control, applying chemicals only when V tends to increase above ξk and suspending application when V tends to decrease. Ecologically, this represents a forced dynamic equilibrium in which control pressure exactly balances the growth rate of the parasite population. Finally, this regime can be regarded as energetically efficient from a management perspective, as it minimizes chemical usage while keeping infestation under control.

In our system, trajectories reach the stable sliding set Σ^{ss}, which represents the region of long–term sustainable management of the apicultural system. Biologically, this means that an optimal intervention regime exists: The infestation level is maintained at the critical threshold without undergoing violent oscillations between crisis states $V >> \xi k$ and treatment-free periods $V << \xi k$. This state is desirable in apicultural practice because it minimizes chemical stress on he bees (avoiding cumulative toxicity) while preventing a collapse due to excessive infestation. From an evolutionary perspective, it may represent an adaptive tolerance strategy in which the colony coexists with a manageable parasitic load.

Within the stable sliding region, trajectories converge to the pseudoequilibrium, which represents a stationary state of integrated management in which the three variables (A, V, M) stabilize under

intermittent chemical control. This implies that the bee population A reaches a stable level (generally lower than the carrying capacity k due to the energetic cost of coexisting with $V \approx \xi k$), the mite population V is maintained exactly at the critical threshold ξk, and honey production M reaches an equilibrium level (reduced relative to the parasite-free case, but maximal given the infestation level). Biologically, this represents a long-term management strategy in which the beekeeper accepts a constant parasitic load at the critical threshold, thereby avoiding both colony collapse and excessive chemical use.

3.3. Numerical simulations of the piecewise smooth model

To graphically illustrate the dynamic behavior analytically described in the previous subsection and to validate the theoretical results obtained, numerical simulations are performed by considering initial conditions that are strategically distributed across the different regions S_1 and S_2 of the state space, using parameter values taken from Table 1, as shown in Figure 6. The numerical simulations were implemented using an integration algorithm in Matlab adapted for piecewise smooth systems, which accurately captures the transitions between regions and the behavior on the discontinuity surfaces.

The results of the simulations clearly show that the system's trajectories, regardless of their specific initial conditions within each region, exhibit a characteristic convergent behavior toward the switching surface Σ. It is evident that all trajectories initially pass through the crossing set Σ^c, where the vector field undergoes discontinuous transitions between the subsystems associated with regions S_1 and S_2. This transient behavior confirms the attractive nature of the stable sliding region Σ^{ss} for the range of parameters considered in the study.

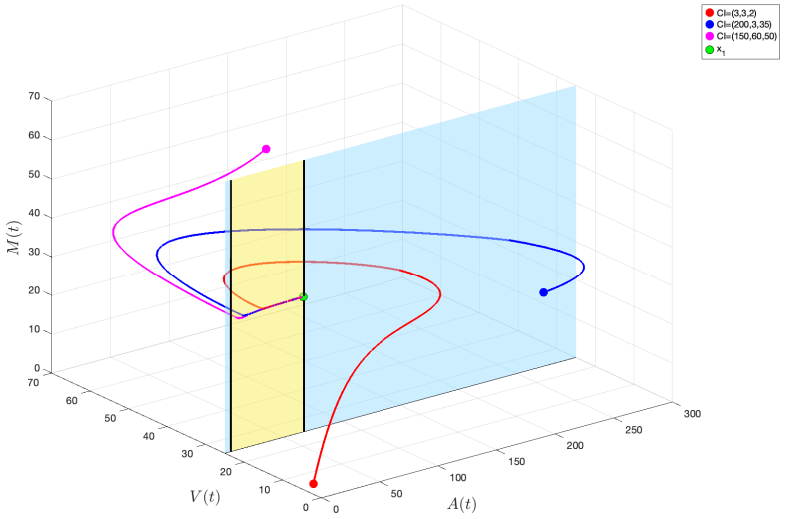

Figure 6. Phase portrait of the system (3.3). The pseudo-equilibrium is shown in green and the initial conditions are in the regions S_1 and S_2.

Particularly noteworthy is the behavior observed when the trajectories reach the sliding region Σ^s,

where the system exhibits the phenomenon of sliding modes characteristic of Filippov systems. In this region, the sliding solutions evolve on the switching surface following the dynamics defined by the Filippov vector field, constructed via the Filippov convention, and asymptotically approach the pseudo–equilibrium previously identified through our theoretical analysis, which is illustrated in green. The convergence observed in the simulations toward this point confirms its local stability both numerically and graphically, thereby validating the analytical predictions derived from the study of the Jacobian matrix of the reduced system.

Numerical simulations also enable a visualization of the robustness of the system's behavior with respect to variations in the initial conditions, demonstrating that the pseudo–equilibrium acts as a local attractor within the sliding region. This result has important implications from an apicultural management perspective, as it suggests that the system naturally tends toward a stable equilibrium state involving the bee population, parasite load, and honey production, regardless of the initial fluctuations in these variables. The stability of the pseudo–equilibrium ensures the effectiveness of the chemical control protocol implemented via the switching term, providing a solid foundation for the design of management strategies that maintain mite infestations within biologically and economically acceptable thresholds.

Furthermore, to complement the previous analysis and specifically study the dynamic behavior over the sliding region, additional numerical simulations are performed, as illustrated in Figure 7, where the initial conditions are placed directly on Σ^s. This experimental setup allows for the isolation and a detailed examination of the sliding mode behavior without the influence of the transient dynamics associated with the vector fields f_1 and f_2 defined on regions S_1 and S_2, respectively.

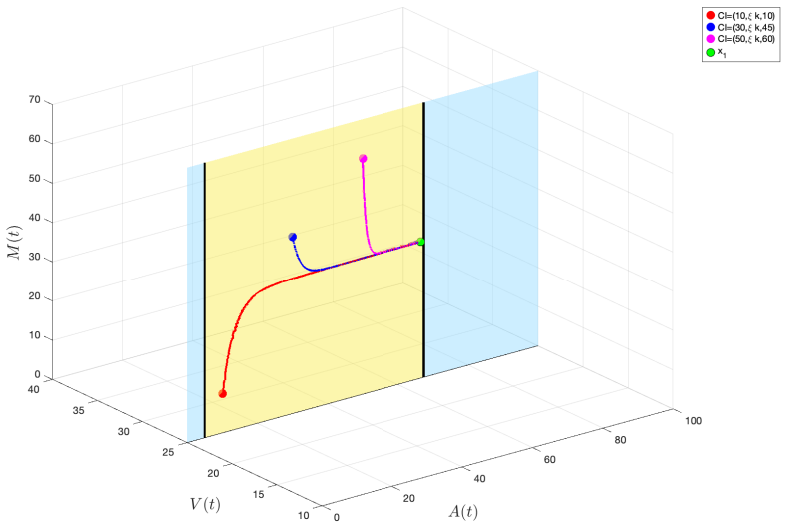

Figure 7. Phase portrait of the system (3.3). The pseudo–equilibrium is shown in green, and the initial conditions are in the set of slip points Σ^s.

The simulations show that when the system starts within the sliding region, the trajectories follow

the sliding behavior predicted by the Filippov vector field, which is obtained through the convex combination of the vector fields adjacent to the discontinuity surface. This vector field defines the reduced dynamics on Σ^s and governs the temporal evolution of the system when it is confined to the sliding region. In particular, it is once again confirmed that all trajectories converge toward the analytically identified pseudo–equilibrium.

From a biological perspective, these results have significant implications for the interpretation of the proposed model. The observed sliding behavior suggests that once the chemical control protocol is activated (i.e., when the system reaches the sliding region Σ^s), the system evolves deterministically toward a controlled equilibrium state, characterized by specific levels of the bee population, parasite load, and honey production. The stability of the pseudo–equilibrium ensures that small perturbations in these variables will not compromise the effectiveness of the control protocol, as the system will naturally return to the desired equilibrium state.

4. Discussion

The proposed mathematical model, based on a system of first–order nonlinear ordinary differential equations, constitutes a suitable tool for describing host–parasitoid–type interactions, as demonstrated by classical studies in mathematical ecology [42, 43]. Both in its smooth version (2.1) and in its piecewise smooth formulation (3.3), the model presented in this work is original and accurately reflects the expected dynamics in beekeeping systems affected by the *Varroa destructor* mite. Its construction is based on realistic and widely accepted assumptions in the mathematical ecology literature, thereby reinforcing the validity of the adopted approach. The results obtained are consistent with the agroecological principles that govern the sustainable management of honey bee colonies, and the mathematical propositions developed, which establish the biological feasibility and local stability conditions, as well as the qualitative analysis of the nonsmooth system using Filippov theory, are supported by a rigorous and well-structured formulation. Moreover, particular care has been taken to interpret each result from a biological and productive perspective, connecting the mathematical theory with its ecological and practical relevance.

The qualitative analysis of the smooth model (2.1) revealed that the population dynamics are strongly conditioned by the critical thresholds A_0 and U, which determine the biological feasibility of the equilibrium points E_2 and E_3 (Proposition 1), as well as the stability of all equilibrium points of the system (Propositions 2–4). Since these thresholds can be expressed in terms of the parameter q_1, and considering that this parameter represents the bee mortality rate due to exposure to insecticides applied in crops adjacent to the beekeeping ecosystem (a quantity that can be modified by beekeeping practices), we systematically varied its value in the numerical simulations. This decision made it possible to illustrate how different levels of chemical intervention affect the qualitative behavior of the system. In particular, when insecticide-induced mortality (q_1) is high, the system collapses to the trivial equilibrium $E_1 = (0, 0, 0)$, which implies the extinction of both bees and mites and the complete loss of honey production. This result highlights the negative impact of excessive chemical pressure on the beekeeping ecosystem.

In contrast, when q_1 remains at moderate levels, the system converges to an ecologically favorable equilibrium represented by E_2, where bees persist and honey production is sustained in the absence of mites. This finding underscores the importance of prudent use of insecticides, allowing the bee

population to recover, alongside and productive restoration of the system.

Finally, under low chemical intervention scenarios, the system exhibits the stable coexistence of bees, mites, and honey production, represented by the equilibrium point E_3, which is locally and asymptotically stable. This outcome highlights the possibility of natural ecological control, where the mite population remains within tolerable limits without significantly compromising honey production. From an agroecological perspective, this scenario raises important questions regarding the necessity of chemical intervention in contexts where the system is capable of self-regulation.

In the case of the piecewise smooth model (3.3), the analysis based on Filippov theory and the associated simulations show that upon introducing a threshold that activates the switching term based on the infestation ratio, the system evolves toward a stable pseudo–equilibrium within the sliding region. This behavior indicates that the targeted activation of chemical control strategies, conditioned by the infestation level, allows the population dynamics to stabilize under a sustainable regime, preventing both the collapse of the bee population and the uncontrolled proliferation of the mite. In summary, the results suggest that the use of piecewise smooth models with threshold–activated control enhances both the realism and the applicability of the model, aligning with current apicultural management practices based on monitoring.

Limitations

One of the main limitations of the present study is the use of hypothetical values for the model's parameters. Although these values allow the illustration of different dynamic scenarios and support qualitative analyses, they do not necessarily reflect the actual conditions of a specific beekeeping ecosystem. This limitation compromises the applicability of the model as a deterministic tool for faithfully describing the temporal evolution of the system in an empirical context, particularly regarding the estimation of critical thresholds or the precise evaluation of control strategies.

In particular, the parameter k, which represents the carrying capacity of the bee population, was not calibrated using empirical data, since the geographical or ecological context of the studied population was not specified throughout the manuscript. The model may represent either a single hive or an entire apiary, but it lacks validation based on observational data. Therefore, a natural extension of this work involves conducting statistical studies to fit the parameters using experimental or field data, thereby increasing the accuracy and applicability of the deterministic model to real-world scenarios.

From a threshold–based perspective, the threshold U, which determines qualitative transitions in the dynamics of the system (2.1), depends nonlinearly on the parameters associated with both insecticide exposure and the colony's resilience. The sensitivity of this threshold to parameter uncertainty can be analyzed through the concept of elasticity, which, for a generic parameter θ, is defined as

$$E_\theta = \frac{\theta}{U}\frac{\partial U}{\partial \theta},$$

and measures the relative change in the threshold induced by a relative variation in the parameter. According to this analysis, it is observed that U exhibits positive elasticities with respect to parameters such as k, β, σ, and ε, indicating that relative increases in these parameters tend to increase the value of the threshold. In contrast, parameters associated with mortality or loss processes, such as μ, q_1, q_2, and ω, display negative elasticities, contributing to a decrease in the critical threshold.

Consequently, uncertainty in parameter estimation may shift the position of the threshold U and modify the location and extent of the basins of attraction in the phase space. Nevertheless, these

variations do not alter the fundamental qualitative structure of the dynamics but affect the location of the thresholds that separate distinct system behaviors. The use of elasticities as a tool to interpret the relative influence of parameters on threshold quantities is a well-established approach in the mathematical biology and population dynamics literature, both in epidemiological and ecological models [44, 45].

Future work

Regarding the smooth model, a future direction involves conducting a rigorous bifurcation analysis by analytically demonstrating their occurrence using tools such as Sotomayor's theorem [46]. Indeed, the results obtained suggest the presence of transcritical bifurcations at the equilibrium points E_1 and E_2 when the parameter q_1 crosses the critical value q_1^*, as well as between the points E_2 and E_3 when q_1 crosses q_1^{**}. This analysis would deepen the understanding of qualitative changes in the system's dynamics and characterize transitions between ecological regimes.

Concerning the piecewise smooth model (3.3), two complementary future research directions are proposed. First, it is possible to define the sliding dynamics using a variation of the convex combination of the vector fields adjacent to the switching surface, known as the convex Filippov method. Although this is a standard tool for defining sliding systems, such as in (3.7), alternative approaches allow for a more general characterization. One such approach involves introducing nonlinear sliding dynamics. This method proposes adding a term G to the traditionally defined linear Filippov sliding dynamics, resulting in a generalized definition of the sliding phenomenon. The inclusion of this nonlinear term is crucial, as it gives rise to what some authors refer to as hidden dynamics [47]. These dynamics, which are not captured by the linear model, are essential for understanding the nature of transition quantities, offering a more comprehensive representation of the system's complexity within the sliding set.

Second, it is suggested to model honey harvesting not as a continuous process with a constant rate, but rather as an action conditioned on exceeding a honey accumulation threshold. This proposal would lead to a new piecewise smooth system in which the switching variable depends on the amount of honey M, thus enabling a more realistic representation of beekeeping practices that avoid overharvesting and protect the colony's health. A preliminary example of this modification is the following:

$$\frac{dM}{dt} = \rho A - \delta A M - \theta \alpha M,$$

where

$$\theta = \begin{cases} 0 & \text{si} \quad M < m \\ 1 & \text{si} \quad M > m, \end{cases} \tag{4.1}$$

and m represents the maximum amount of honey that can be extracted from the beekeeping ecosystem without compromising its stability. This formulation allows modeling of management strategies in which honey harvesting is carried out prudently and conditionally, with the goal of preserving the colony's health and long-term sustainability. For instance, [48] provides specific recommendations regarding the amount of honey that should be left in the hive, which depend on factors such as climate and the length of the winter season.

Use of AI tools declaration

During the preparation of this work, the authors used GPT-5.2 to assist with language editing and improvement of the English text. The AI tool was not used to generate scientific content, develop

the mathematical model, perform analyses, or draw conclusions. All scientific responsibility for the content of the manuscript remains with the authors.

Acknowledgments

The authors of this paper would like to thank the Corporación Universitaria Empresarial Alexander von Humboldt for its support within the framework of the research project entitled "Mathematical model of the impact of varroosis on honey production".

Conflict of interest

The authors declare there is no conflict of interest.

References

1. A. Klein, B. Vaissière, J. Cane, I. Steffan-Dewenter, S. Cunningham, C. Kremen, et al., Importance of pollinators in changing landscapes for world crops, *Proc. R. Soc. B*, **274** (2007), 303–313. https://doi.org/10.1098/rspb.2006.3721
2. N. Gallai, J. Salles, J. Settele, B. Vaissière, Economic valuation of the vulnerability of world agriculture confronted with pollinator decline, *Ecol. Econ.*, **68** (2009), 810–821. https://doi.org/10.1016/j.ecolecon.2008.06.014
3. S. Potts, V. Imperatriz-Fonseca, H. Ngo, M. Aizen, J. Biesmeijer, T. Breeze, et al., Safeguarding pollinators and their values to human well-being, *Nature*, **540** (2016), 220–229. https://doi.org/10.1038/nature20588
4. A. Vanbergen, Insect pollinators initiative, threats to an ecosystem service: Pressures on pollinators, *Front. Ecol. Environ.*, **11** (2013), 251–259. https://doi.org/10.1890/120126
5. D. Goulson, E. Nicholls, C. Botías, E. Rotheray, Bee declines driven by combined stress from parasites, pesticides, and lack of flowers, *Science*, **347** (2015), 1255957. https://doi.org/10.1126/science.1255957
6. F. Sanchez-Bayo, K. Goka, Pesticide residues and bees – a risk assessment, *PLoS One*, **9** (2014), e94482. https://doi.org/10.1371/journal.pone.0094482
7. P. Martínez-Álvarez, H. Toro-Zapata, G. Salcedo-Echeverry, Population dynamics of a honeybee colony *Apis mellifera* under pesticide-induced environmental stress, *Theor. Ecol.*, **18** (2025), 1–25. https://doi.org/10.1007/s12080-025-00623-w
8. M. El Hajji, F. Alzahrani, M. Alharbi, Mathematical analysis for honeybee dynamics under the influence of seasonality, *Mathematics*, **12** (2024), 3496. https://doi.org/10.3390/math12223496
9. P. Rosenkranz, P. Aumeier, B. Ziegelmann, Biology and control of *Varroa destructor*, *J. Invertebr. Pathol.*, **103** (2010), S96–S119. https://doi.org/10.1016/j.jip.2009.07.016
10. D. van Engelsdorp, J. Evans, C. Saegerman, C. Mullin, E. Haubruge, B. K. Nguyen, et al., Colony collapse disorder: A descriptive study, *PLoS One*, **4** (2009), e6481. https://doi.org/10.1371/journal.pone.0006481

11. N. Steinhauer, K. Kulhanek, K. Antúnez, H. Human, P. Chantawannakul, M. Chauzat, et al., Drivers of colony losses, *Curr. Opin. Insect Sci.*, **26** (2018), 142–148. https://doi.org/10.1016/j.cois.2018.02.004
12. D. Anderson, J. Trueman, *Varroa jacobsoni* (Acari: Varroidae) is more than one species, *Exp. Appl. Acarol.*, **24** (2000), 165–189. https://doi.org/10.1023/A:1006456720416
13. L. Wilfert, G. Long, H. Leggett, S. Martin, P. Schmid-Hempel, R. Butlin, et al., Deformed wing virus is a recent global epidemic in honeybees driven by *Varroa* mites, *Science*, **351** (2016), 594–597. https://doi.org/10.1126/science.aac9976
14. S. Martin, The role of *Varroa* and viral pathogens in the collapse of honeybee colonies: A modelling approach, *J. Appl. Ecol.*, **38** (2001), 1082–1093. https://doi.org/10.1046/j.1365-2664.2001.00662.x
15. Y. Le Conte, M. Ellis, W. Ritter, *Varroa* mites and honey bee health: Can *Varroa* explain part of the colony losses, *Apidologie*, **41** (2010), 353–363. https://doi.org/10.1051/apido/2010017
16. C. Holling, Resilience and stability of ecological systems, in *Foundations of Socio-Environmental Research: Legacy Readings with Commentaries*, Cambridge University Press, (1973), 1–23.
17. R. May, Simple mathematical models with very complicated dynamics, *Nature*, **261** (1976), 459–467. https://doi.org/10.1038/261459a0
18. H. Barclay, Models for pest control using predator release, habitat management and pesticide release in combination, *J. Appl. Ecol.*, **19** (1982), 337–348.
19. R. Sutherst, G. Maywald, A climate model of the red imported fire ant, *Solenopsis invicta* Buren (Hymenoptera: Formicidae): Implications for invasion of new regions, particularly Oceania, *Environ. Entomol.*, **34** (2005), 317–335. https://doi.org/10.1603/0046-225X-34.2.317
20. M. Scheffer, S. Carpenter, J. Foley, C. Folke, B. Walker, Catastrophic shifts in ecosystems, *Nature*, **413** (2001), 591–596. https://doi.org/10.1038/35098000
21. A. Atanasov, S. Georgiev, L. Vulkov, Parameters reconstruction in modeling of honeybee colonies infested with *Varroa destructor*, in *AIP Conference Proceedings*, (2022), 110005. https://doi.org/10.1063/5.0101040
22. G. DeGrandi-Hoffman, R. Curry, A mathematical model of *Varroa* mite (*Varroa destructor* Anderson and Trueman) and honeybee (*Apis mellifera* L.) population dynamics, *Int. J. Acarol.*, **30** (2004), 259–274. https://doi.org/10.1080/01647950408684393
23. A. Dénes, M. Ibrahim, Global dynamics of a mathematical model for a honeybee colony infested by virus-carrying *Varroa* mites, *J. Appl. Math. Comput.*, **61** (2019), 349–371. https://doi.org/10.1007/s12190-019-01250-5
24. M. Ibrahim, A. Dénes, A mathematical model for the spread of *Varroa* mites in honeybee populations: Two simulation scenarios with seasonality, *Heliyon*, **8** (2022), e10648. https://doi.org/10.1016/j.heliyon.2022.e10648
25. D. Wilkinson, G. Smith, A model of the mite parasite, *Varroa destructor*, on honeybees (*Apis mellifera*) to investigate parameters important to mite population growth, *Ecol. Modell.*, **148** (2002), 263–275. https://doi.org/10.1016/S0304-3800(01)00440-9

26. A. Filippov, *Differential Equations with Discontinuous Righthand Sides: Control Systems*, Mathematics and its Applications (Soviet Series), Kluwer Academic Publishers, Dordrecht, 1988.
27. M. Bernardo, C. Budd, A. Champneys, P. Kowalczyk, *Piecewise-smooth Dynamical Systems: Theory and Applications*, Springer Science & Business Media, 2008.
28. S. Tang, L. Chen, Density-dependent birth rate, birth pulses and their population dynamic consequences, *Math. Biol.*, **44** (2002), 185–199. https://doi.org/10.1007/s002850100121
29. S. Zhang, D. Tan, L. Chen, Chaos in periodically forced Holling type II predator-prey system with impulsive perturbations, *Chaos Solitons Fractals*, **28** (2006), 367–376. https://doi.org/10.1016/j.chaos.2005.05.037
30. C. Perry, E. Søvik, M. Myerscough, A. Barron, Rapid behavioral maturation accelerates failure of stressed honey bee colonies, *Proc. Natl. Acad. Sci.*, **112** (2015), 3427–3432. https://doi.org/10.1073/pnas.1422089112
31. J. Liang, S. Tang, Optimal dosage and economic threshold of multiple pesticide applications for pest control, *Math. Comput. Modell.*, **51** (2010), 487–503. https://doi.org/10.1016/J.MCM.2009.11.021
32. R. Ripa, P. Larral, *Manejo de Plagas en Paltos y Cítricos*, Colección de libros INIA No 23, Instituto de Investigaciones Agropecuarias del Ministerio de Agricultura de Chile, La Cruz (Chile), 2008.
33. C. Barril, A. Calsina, S. Cuadrado, J. Ripoll, On the basic reproduction number in continuously structured populations, *Math. Methods Appl. Sci.*, **44** (2021), 799–812. https://doi.org/10.1002/mma.6787
34. Y. Kuznetsov, *Elements of Applied Bifurcation Theory, Applied Mathematical Sciences*, Springer-Verlag, New York, 2023. https://doi.org/10.1007/978-3-031-22007-4
35. R. Leine, H. Nijmeijer, *Dynamics and Bifurcations of Non-smooth Mechanical Systems*, Springer Science & Business Media, 2004. https://doi.org/10.1007/978-3-540-44398-8
36. K. Delaplane, J. van der Steen, E. Guzman-Novoa, Standard methods for estimating strength parameters of *Apis mellifera* colonies, *J. Apic. Res.*, **52** (2013), 1–12. https://doi.org/10.3896/IBRA.1.52.1.03
37. M. Branco, N. Kidd, R. Pickard, A comparative evaluation of sampling methods for *Varroa destructor* (Acari: Varroidae) population estimation, *Apidologie*, **37** (2006), 452–461. http://doi.org/10.1051/apido:2006010
38. V. Dietemann, F. Nazzi, S. Martin, D. Anderson, B. Locke, K. Delaplane, et al., Standard methods for varroa research, *J. Apic. Res.*, **52** (2013), 1–54. https://doi.org/10.3896/IBRA.1.52.1.09
39. J. Strange, W. Sheppard, Optimum timing of miticide applications for control of *Varroa destructor* (Acari: Varroidae) in *Apis mellifera* (Hymenoptera: Apidae) in Washington State, USA, *J. Econ. Entomol.*, **94** (2001), 1324–1331. https://doi.org/10.1603/0022-0493-94.6.1324
40. A. Colombo, M. di Bernardo, S. Hogan, M. Jeffrey, Bifurcations of piecewise smooth flows: Perspectives, methodologies and open problems, *Physica D: Nonlinear Phenom.*, **241** (2012), 1845–1860. https://doi.org/10.1016/j.physd.2011.09.017

41. O. Molina-Díaz, G. Olivar-Tost, D. Sotelo-Castelblanco, Fold-Fold singularity in a piecewise smooth mathematical model describing the dynamics of a stockless market, *Mathematics*, **12** (2024), 2442. https://doi.org/10.3390/math12162442
42. J. Murray, *Mathematical Biology I: An Introduction*, Springer-Verlag, New York, 2002. https://doi.org/10.1007/b98868
43. M. Kot, *Elements of Mathematical Ecology*, Cambridge University Press, Cambridge, 2001.
44. N. Chitnis, J. Hyman, J. Cushing, Determining important parameters in the spread of malaria through the sensitivity analysis of a mathematical model, *Bull. Math. Biol.*, **70** (2008), 1272–1296. https://doi.org/10.1007/s11538-008-9299-0
45. L. Arriola, J. Hyman, Sensitivity analysis for uncertainty quantification in mathematical models, in *Mathematical and Statistical Estimation Approaches in Epidemiology*, Springer, Dordrecht, (2009), 195–247. https://doi.org/10.1007/978-90-481-2313-1_10
46. L. Perko, *Differential Equations and Dynamical Systems*, Springer Science & Business Media, New York, 2001.
47. D. Novaes, M. Jeffrey, Regularization of hidden dynamics in piecewise smooth flow, *J. Differ. Equ.*, **259** (2015), 4615–4633. https://doi.org/10.1016/j.jde.2015.06.005
48. C. Bir, C. Lucas, Beekeeping-honey harvest methods, costs and breakeven calculations, Oklahoma Cooperative Extension Service, Oklahoma State University, 2022.

AIMS Press